Advanced Functional Materials XX (2010) XXX
DOI: 10.1002/adfm.201001650

Highly Conductive Redox Protein-Carbon Nanotube Complex for Biosensing Applications

Chiara Baldacchini[1,2,*], *Maria Antonia Herrero Chamorro*[3,+], *Maurizio Prato*[3], and *Salvatore Cannistraro*[1]

[1] Biophysics and Nanoscience Centre and CNISM, Facoltà di Scienze, Università della Tuscia, Largo dell'Università, 01100, Viterbo (Italy).
[2] Institute of Agro-environmental and Forest Biology – IBAF, National Research Council – CNR, Via Marconi 2, 05010 Porano, TR (Italy).
[3] Dipartimento di Scienze Farmaceutiche, Università di Trieste, Piazzale Europa 1, 34127 Trieste (Italy).

Keywords: Bioelectronics, Bionanotechnology, Carbon Nanotubes, Charge Transport

The integration of redox proteins with nanomaterials has attracted much interest in the last years, and metallic single-walled carbon nanotubes have been introduced as efficient electrical wires, to connect biomolecules to metal electrodes in advanced nano-biodevices. Besides preserving biofunctionality, the protein-nanotube connection should ensure appropriate molecular orientation, flexibility, and efficient, reproducible electrical conduction. In this respect, we connect yeast cytochrome c redox proteins to gold electrodes through lying-down functionalized metallic single-walled carbon nanotubes. Immobilization of cytochromes to nanotubes is obtained *via* covalent bond between the exposed protein thiols and maleimide-terminated functional chains attached to the carbon nanotubes. A single-molecule study performed by combining scanning probe nanoscopies ascertains that the protein topological properties are preserved upon binding and provides unprecedented current images of single proteins bound to carbon nanotubes that allow a detailed I-V characterization. Collectively, the results point out that the use as linkers of suitably functionalized metallic SWNTs results in an electrical communication between redox proteins and gold electrodes more efficient and reproducible than for proteins directly connected with metal surfaces.

1. Introduction

Hybrid systems obtained by conjugating redox proteins with nanomaterials deserve particular interest for application in bioelectronics, biosensing and biofuel cells.[1-3] On one side, redox proteins are nanoscaled objects able to produce processable signals in response to biorecognition events, environment modifications or optical absorption, due also to their electron transfer properties.[4,5] On the other, suitably functionalized organic and inorganic nanostructures (carbon nanotubes, metal nanoparticles or semiconducting quantum dots) can act as efficient transducers of tiny signals from biological elements towards macroscopic electrodes, since their peculiar low-dimension physical and chemical properties enable more efficient and less noisy channels with respect to bulk materials.[6] In this context, design and development of nano-biodevices coupling redox proteins with single-walled carbon nanotubes (SWNTs) have extraordinarily grown. Many strategies have been employed to conjugate redox proteins with SWNTs: non-covalent adsorption,[7,8] electrostatic interaction,[9-14] π-stacking modification,[15] and covalent functionalization[10,16-20] have been exploited. Such a coupling should meet a

number of crucial requirements: (i) the protein functionality has to be preserved; (ii) the protein orientation towards the environment has to be properly controlled, in order to facilitate the exposition of the active site; (iii) the proteins should be endowed with sufficient reorientational diffusional freedom, to favor the biorecognition process; (iv) an efficient electrical conduction across the protein-nanotube-electrode system has to be established.

Most of the immobilization protocols used in previous works to integrate redox proteins with carbon nanotubes exploit the abundant $-NH_2$ groups, which are randomly distributed on the biomolecular surfaces, and, therefore, do not permit an univocal protein orientation. SWNTs functionalized with organic chains exposing reacting terminations able to selectively bind organic groups already present, or suitably engineered, on protein surfaces, such as thiols, should be preferred.

In this connection, we performed a nanoscopic topological and electrical characterization of a prototype system consisting of SWNTs covalently functionalized with maleimide-terminated chains (Mal-SWNTs)[21] conjugated with yeast cytochrome c (YCC) redox proteins (Figure S1, S2, S3 in Supporting Information, SI). The thiol group belonging to the single exposed cysteine of YCC, which is located in the region opposite to the lysine-rich protein docking site, should covalently react with malemide, ensuring a strong, oriented nanotube-protein bond that leaves the docking site free to interact. Topological and functional properties of cytochrome c coupled with SWNTs have been already described, with nano-biosensor application aims.[7-14,20] Nevertheless, no attention has been paid to achieve simultaneous control of the protein orientation and of the protein-nanotube electrical connection. By means of a multitechnique approach based on scanning tunneling microscopy (STM) and conductive atomic force microscopy (C-AFM), unprecedented stable and high-resolution current images of single YCC molecules bound to metallic Mal-SWNTs lying on gold electrodes have been obtained. This allowed to perform a detailed current-voltage (I-V) characterization at the single molecule level, which demonstrated that the use of metallic Mal-SWNTs renders the electrical communication between YCC and gold more efficient, stable and reproducible with respect to that corresponding to proteins chemisorbed at the metal surface.

2. Results and discussion

A typical Tapping Mode AFM (TM-AFM) image of a maleimide-functionalized nanotube lying on a gold surface is shown in Figure 1a. Mal-SWNTs have a mean diameter of 1.5 ± 0.7 nm and a mean length of about 150 nm, consistently with the pristine SWNTs nominal diameter (1-2 nm) and with a shortening due to the acid treatment (pristine SWNTs are 1-2 μm long). Along their length, lumps less than 1 nm high and with a linear density of 32 ± 11 μm^{-1} are visible (marked by arrows in Figure 1a). These lumps, which are absent in pristine SWNTs (Figure S4, SI), are attributed to the maleimide-terminated functional chains covalently attached to the nanotube sidewalls. After incubation with an YCC solution, the flat gold electrode appears covered by a layer of globular objects, which correspond to proteins chemisorbed *via* their exposed thiol,[14,22] and the nanotubes are decorated by lumps (Figure 1b) that have the same linear density (34 ± 11 μm^{-1}) but a larger mean height (2.8 ± 1.1 nm) than those corresponding to the maleimide-terminated functional chains (shown in Figure 1a). Such larger lumps have a mean height that is close to that previously measured by TM-AFM for YCC molecules chemisorbed on bare (2.6

± 0.7 nm)[22] and maleimide-modified (3.1 ± 0.7 nm)[14] gold surfaces. Therefore, they are reasonably attributed to YCC molecules bound to Mal-SWNT sidewalls with native-like topological properties, in a 1:1 ratio with respect to the nanotube functional sites.

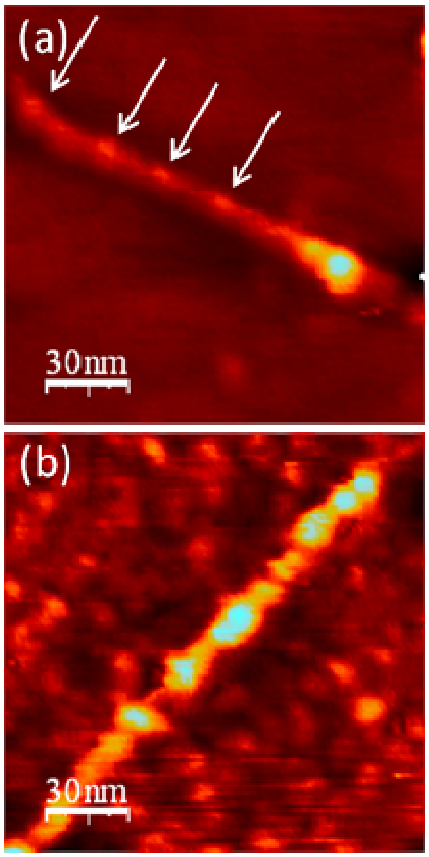

Figure 1. Representative TM-AFM images of MAL-SWNTs taken in air before (a) and after (b) the addition of YCC molecules (image size 150 x 150 nm^2, color range 4 nm). Lumps ascribed to maleimide-terminated functional chains are marked by arrows in panel a.

The electrical properties of the cytochrome-nanotube system have been investigated by means of both STM and C-AFM (Figure S3, SI). Since we are interested in maximizing the electrical communication between proteins and metal electrodes, we selected as linkers metallic SWNTs, which are generally mixed with semiconducting ones in commercial samples. Such discrimination has been done by measuring the nanotube density of states (in STM)[23] and the nanotube current response as a function of an applied load (in C-AFM)[24].

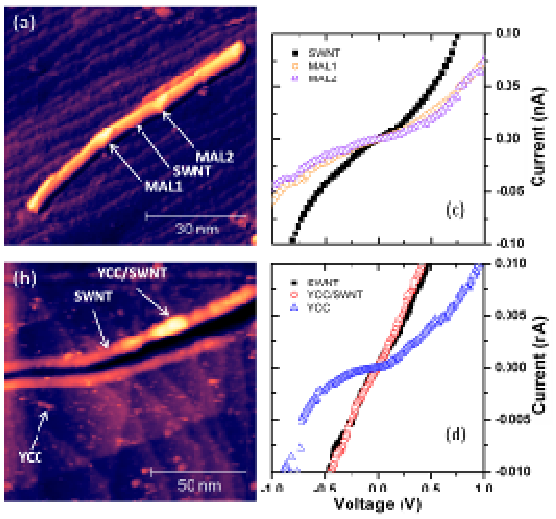

Figure 2. Representative STM images (a,b) and I-V characteristics (c,d) of metallic Mal-SWNTs before (a,c; image and engage parameters: V_b = 0.4 V, I_t = 40 pA, scan rate 6.1 Hz, vertical range 2.5 nm) and after (b,d; image and engage parameters: V_b=-1.5 V, I_t = 26 pA, scan rate 3.8 Hz, vertical range 4.5 nm) the addition of YCC molecules. The shown I-V curves have been measured at the points indicated by the arrows.

Representative STM images of metallic Mal-SWNTs, taken before and after the incubation with an YCC solution, are shown in Figure 2a and Figure 2b, respectively. Before protein deposition, the maleimide-terminated chains are imaged on nanotube sidewalls as bright lumps about 1 nm high (Figure 2a), as generally observed for functional groups covalently attached to SWNTs.[25-27] After protein deposition, the lumps ascribed to YCC molecules are visible both along the nanotubes and on the gold electrode (Figure 2b). Interestingly, proteins chemisorbed on gold appear much smaller than their real dimensions (0.8 ± 0.4 nm),

as previously observed,[28] while cytochromes bound to Mal-SWNTs show a mean height of 2.8 ± 0.8 nm, fairly similar to the real one. STM topography may depend on the conduction properties of the imaged structures, since it is obtained by controlling the tip to sample distance as a function of the electron current tunneling between them: conductive objects (such as metallic carbon nanotubes or metal nanoparticles) are imaged almost with their real dimensions, while the physical height of dielectric systems (such as biomolecules) is generally underestimated.[29] Accordingly, the larger molecular height of YCC molecules bound to metallic Mal-SWNTs displays that they are much more conductive than cytochromes directly chemisorbed on metal electrodes.

The good resolution achieved in STM images and the high instrumental stability allowed to position the STM tip on top of single nanotubes, maleimide-terminated functional sites and proteins (see Figure S3, SI), and to measure the current tunneling across such structures as a function of the applied bias (I-V spectroscopy), which is proportional to the local density of states. In particular, our investigation focused on metallic Mal-SWNTs, whose I-V characteristics are symmetric and linearly increasing, without conduction gap, at low bias (square marks in Figure 2c and Figure 2d, measured at the points marked as SWNT in Figure 2a and 2b, respectively). The I-V curves measured on top of maleimide-terminated functional chains attached to metallic Mal-SWNTs (MAL1 and MAL2 in Figure 2a, circle and triangle marks in Figure 2c, respectively) and on top of YCC molecules bound to them (YCC/SWNT in Figure 2b and circle marks in Figure 2d) are slightly asymmetric (more intense at positive bias) but still linear at low applied bias, confirming that a transverse (i.e., perpendicular to the main nanotube axis)[24] metallic-like conduction channel is active across the hybrid systems. At variance, the current signal measured on top of YCC molecules chemisorbed at the gold electrode (YCC in Figure 2b, triangle marks in Figure 2d) is sigmoidal-shaped, as expected for dielectric materials, and much less intense than that measured across the cytochrome-nanotube system.

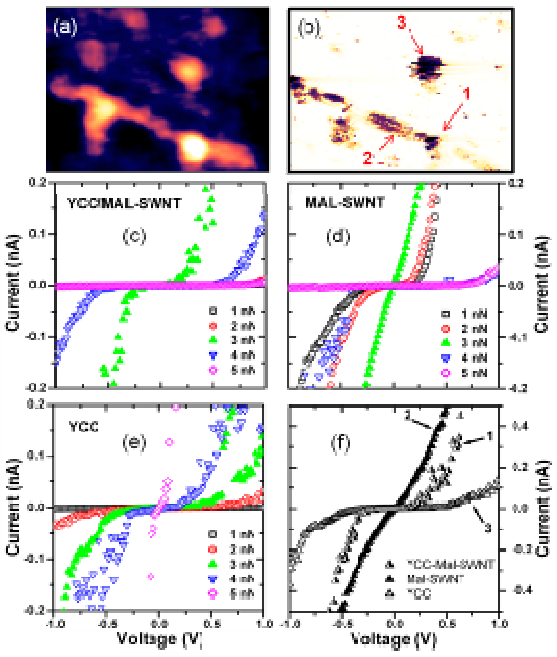

Figure 3. C-AFM topography (a) and current (b) images of a metallic Mal-SWNT on a gold surface after the addition of YCC molecules (image size = 240 x 175 nm^2, F = 1.0 nN, V_b = -1.0 V, scan rate 1.8 Hz, color range 2 nm and 10 nA, respectively). Arrows indicate the points at which the I-V curves shown in panel c-f have been measured: an YCC molecule bound to the Mal-SWNT (arrow 1, panel c), a bare section of the Mal-SWNT (arrow 2, panel d) and an YCC molecule chemisorbed at the gold surface (arrow 3, panel e). Panel f shows the comparison among the three I-V curves measured by applying a force of 3 nN.

To get additional insights into the conduction mechanism of the cytochrome-nanotube system, C-AFM measurements have been performed, since they are able to

map the morphological and conductive properties of a sample while establishing a real physical contact with it, without tunneling gap (see Figure S3, SI). Representative topography and current images of a metallic Mal-SWNT with bound YCC molecules are shown in Figure 3a and Figure 3b, respectively. Clear current maps have been obtained for a number of protein-nanotube systems, at both negative and positive applied bias and after repetitive scans. At variance, proteins chemisorbed on gold (such as those shown in the upper region of Figure 3a,b) show variable current contrasts, probably owing to uncontrolled, additional interactions with respect to S-Au bond, as previously observed for mutant plastocyanin molecules.[30] It is worth noting that the striking one-to-one correspondence obtained between morphological and conductive images of cytochromes bound to metallic Mal-SWNTs is unprecedented for biological materials. Indeed, clear correlation between C-AFM topography and current maps has been obtained only for inorganic[31] and organic[24,32] nanostructures, while it has been hardly achieved for biomolecules.[30] This is probably due to adhesion and capillary forces arising at soft biological surfaces, which hamper a fine tuning of the force applied by the tip. However, load tuning is crucial to optimize the tip-to-molecule electrical contact avoiding, at the same time, the molecular deformation. To get a deeper insight into this aspect, the current response of cytochrome-coated metallic Mal-SWNTs has been studied at different applied forces. Representative I-V curves measured on top of the protein marked by arrow 1 in Figure 3b are shown in Figure 3c. The current measured across the protein-nanotube system is maximum at a load of 3 nN and much lower otherwise. For comparison, I-V curves measured on a bare section of the nanotube (arrow 2) and on a cytochrome bound to gold (arrow 3), at the same applied loads, are shown in Figure 3d and Figure 3e, respectively. The current measured across the metallic Mal-SWNT is also maximized when a force of 3 nN is applied, while the current flowing across the protein chemisorbed on gold monotonically increases with raising the force, as previously observed,[30,33] due to the reduction of the tunneling length. By comparing the I-V curves measured at a load of 3 nN across the protein-nanotube system, the metallic nanotube and the cytochrome bound to gold (Figure 3f), it is remarked that hybrid system and metallic Mal-SWNT show similarly intense current responses (1,2), while the current measured across the protein chemisorbed on gold (3) is much less intense and sigmoidal-shaped. Thus, once bound to metallic Mal-SWNTs, YCC molecules are able to sustain intense current signals even when low contact forces are applied, achieving a good protein-electrode electrical communication without any risk of protein deformation. Moreover, the nanotube current response is ohmic-like, confirming that its electronic structure is not locally unperturbed, while a gap opens at low bias in the current signal measured across the hybrid system, suggesting the existence of an interplay between nanotube band-like conduction and electron tunneling across the protein.

3. Conclusions

SWNTs have been functionalized with maleimide-terminated functional chains designed to covalently target thiol groups naturally present or suitably engineered on biomolecular surfaces, with the aim of controlling the molecular orientation towards the environment while providing an efficient electrical connection. TM-AFM measurements showed that YCC molecules bind to Mal-SWNTs retaining their topological properties and in an almost 1:1 ratio with respect to the nanotube functional chains. By means of current sensing scanning probe techniques, unprecedented stable and high resolution single-molecule current images of protein-

coated metallic SWNTs have been obtained. Single-molecule spectroscopic investigations demonstrated that the electrical coupling between YCC molecules and gold electrodes is much more stable and efficient when the proteins are immobilized through lying-down metallic Mal-SWNTs, with respect to direct chemisorptions on metal electrodes. This is probably due to the involvement of the nanotube electronic bands in charge transport across the hybrid system. Thus, the covalent, oriented immobilization strategy proposed enhances the signal transduction between electrically active biomolecules, such as YCC redox protein, and metal electrodes, opening promising perspectives for nano-biosensor applications. Further theoretical investigations may help in fully understand the interplay occurring in such hybrid systems between tunneling transport across the protein milieu and band-like conduction within the nanotubes.

4. Experimental

Materials: Chemicals and proteins have been purchased from Sigma-Aldrich and used without further purification. Mal-SWNTs (Figure S1, SI) have been synthesized as previously described [21], and the functionalization procedure has been controlled by Thermo-Gravimetric Analysis and Raman Spectroscopy (Figure S2, SI). To perform single-molecule investigations, Mal-SWNTs have been deposited on Au surfaces, and then YCC solutions have been incubated on the samples (Figure S3, SI).

Tapping-Mode Atomic Force Microscopy: TM-AFM measurements have been performed by using a Veeco Nanoscope IIIa equipped with rectangular silicon cantilevers (k = 40 N m^{-1}; NSC15-NoAl, MikroMasch) for air measurements, and with V-shaped silicon nitride probes (k = 0.5 N m^{-1}; MSNL, Veeco) for measurements in MilliQ water. Images have been analyzed by using WSxM software by Nanotec Electronica [34].

Current-Sensing Scanning Probe Techniques: STM and C-AFM investigations have been carried out by using an Agilent PicoLE 5100 microscope, with final preamplifier sensitivity of 1 nA V^{-1} and current noise level < 5 pA. STM measurements have been done in ambient conditions, with mechanically cut Pt-Ir tips. STM images have been acquired at applied bias V_b in the ±1.5 V range, constant tunneling current I_t in the 30-100 pA range, and scan rate in the 1-10 Hz range, scaling with the image size. STM I-V curves have been obtained by averaging over 200 single sweeps (t = 0.1 s). C-AFM measurements have been done in pure nitrogen atmosphere, with Ti-Pt coated tips (k = 0.08 N m^{-1}; CSC38, MikroMash). C-AFM images have been acquired at V_b in the ±1.5 V range, applied force of 0.5-2.0 nN, and 1-3 Hz scan rate. C-AFM I-V curves are single sweeps (t = 1 s). For both techniques, the overall drift in x–y plane was evaluated to be less than 1 Å s^{-1}, not appreciably affecting tip position during measurements. To check the drift in z-direction, current fluctuations of less than a 1 pA s^{-1} was recorded by disabling the feedback. STM and C-AFM image analysis has been performed by using Gwyddion open source software by Czech Metrology Institute.

Acknowledgements

M.A.H.C. is indebted to the Junta de Comunidades de Castilla-La Mancha (Spain) for a postdoctoral research grant. Supporting Information is available online from Wiley InterScience or from the author.

*corresponding author: baldacchini@unitus.it.

[+]Present address: Departamento de Química Orgánica - IRICA, Facultad de Química, IRICA, Universidad de Castilla-La Mancha, 13071 Ciudad Real (Spain).

[1] B. Willner, E. Katz, I. Willner, *Curr. Op. Biotech.* **2006**, *17*, 589-596.
[2] Y. Wu, S. Hu, *Microchim. Acta* **2007**, *159*, 1-17.
[3] Q. Chi, P. S. Jensen, J. Ulstrup, in *Nanobioelectronics – for Electronics, Biology and Medicine* (Eds: A. Offenhausser and R. Rinaldi), Springer Science **2009**, 183-210.
[4] A. R. Bizzarri, S. Cannistraro, in *Encyclopedia of Condensed Matter Physics* (Eds: G. Bassani, G. Liedl, P. Wyder), Elsevier Ed. **2005**, 361-369.
[5] H. B. Gray, J. R. Winkler, *Biochim. Biophys. Acta* **2010**, *1797*, 1563-1572.
[6] N. L. Rosi, C. A. Mirkin, *Chem. Rev.* **2005**, *105*, 1547-1562.
[7] H. A. Heering, K. A.Williams, S. de Vries, C. Dekker, *Chem. Phys. Chem.* **2006**, *7*, 1705-1709.
[8] D. H. Nagaraju, R. K. Pandey, V. Lakshminarayan, *J. Electroanal. Chem.* **2009**, *627*, 63-68.
[9] J. J. Davis, R. J. Coles, H. A. O. Hill, *J. Electroanal. Chem.* **1997**, *440*, 279-282.
[10] B. R. Azamian, J. J. Davis, K. S. Coleman, C. B. Bagshaw, M. L. H. Green, *J. Am. Chem. Soc.* **2002**, *124*, 12664-12665.
[11] S. Boussaad, N. J. Tao, R. Zhang, T. Hopson, L. A. Nagahara, *Chem. Comm.* **2003**, 1502-1503.
[12] X. Qu, Z. Peng, Y. Wang, S. Dong, *Electroanalysis* **2005**, *17*, 59-64.
[13] N. W. S. Kam, H. Dai, *J. Am. Chem. Soc.* **2005**, *127*, 6021-6026.
[14] I. Delfino, B. Bonanni, L. Andolfi, C. Baldacchini, A. R. Bizzarri, S. Cannistraro, *J. Phys.: Cond. Matt.* **2007**, *19*, 225009.
[15] K. Besteman, J.-O Lee, F. G. M. Wiertz, H. A. Heering, C. Dekker, *Nano Lett.* **2003**, *3*, 727-730.
[16] J. J. Gooding, R. Wibowo, J. Liu, W. Yang, D. Losic, S. Orbons, F. J. Mearns, J. G. Shapter, D. B. Hibbert, *J. Am. Chem. Soc.* **2003**, *125*, 9006-9007.
[17] Y. Lin, F. Lu, Y. Tu, Z. Ren, *Nano Lett.* **2004**, *4*, 191-195.
[18] F. Patolsky, Y. Weizmann, I. Willner, *Angew. Chem. Int. Ed.* **2004**, *43*, 2113-2117.
[19] J. Liu, A. Chou, W. Rahmat, M. N. Paddon-Row, J. J. Gooding, *Electroanalysis,* **2005**, *17*, 38-46.
[20] C. Baldacchini, S. Cannistraro, *J. Nanosci. Nanotech.* **2010**, *10*, 2753-2758.
[21] D. Pantarotto, C. D. Partidos, R. Graff, J. Hoebeke, J.-P. Briand, M. Prato, A. Bianco, *J. Am. Chem. Soc.* **2003**, *125*, 6160-6164.
[22] B. Bonanni, D. Alliata, A. R. Bizzarri, S. Cannistraro, *Chem. Phys. Chem.* **2003**, *4*, 1183-1188.
[23] J. W. G. Wildöer, L. C. Venema, A. G. Rinzler, R. E. Smalley, C. Dekker, *Nature* **1998**, *391*, 59-62.
[24] C. Baldacchini, S. Cannistraro, *Appl. Phys. Lett.* **2007**, *91*, 122103.
[25] D. Bonifazi, C. Nacci, R. Marega, S. Campidelli, G. Ceballos, S. Modesti, M. Meneghetti, M. Prato, *Nano Lett.* **2006**, *6*, 1409-1414.
[26] A. Hirsch, Phys. *Stat. Sol. B* **2006**, *243*, 3209-3212.
[27] J. Zhang, L. Zhang, V. N. Khabashesku, A. R. Barron, K. F. Kelly, *J. Phys. Chem. C* **2008**, *112*, 12321-12325.
[28] B. Bonanni, D. Alliata, L. Andolfi, A. R. Bizzarri, S. Cannistraro, in *Surface Science Research Developments*, (Ed: C. P. Norris), Nova Science Publishers, Inc. **2005**, 1-73.
[29] D. Alliata, L. Andolfi, S. Cannistraro, *Ultramicroscopy* **2004**, *101*, 231-240.
[30] L. Andolfi, S. Cannistraro, *Surf. Sci.* **2005**, *598*, 68-77.
[31] E. Nahum, Y. Ebenstein, A. Aharoni, T. Mokari, U. Banin, N. Shimoni, O. Millo, *Nano Lett.* **2004**, *4*, 103-108.
[32] J. Y. Park, Y. Qui, P. D. Ashby, B. L. M. Hendriksen, M. Salmeron, *J. Chem. Phys.* **2009**, *130*, 114705.
[33] D. N. Axford, J. J. Davis, *Nanotechnology* **2007**, *18*, 145502.
[34] I. Horcas, R. Fernandez, J. M. Gomez-Rodriguez, J. Colchero, J. Gomez-Herrero, A. M. Baro, *Rev. Sci. Instrum.* **2007**, *78*, 013705.

Advanced Functional Materials XX (2010) XXX
DOI: 10.1002/adfm.201001650

Supporting Information

Highly Conductive Redox Protein-Carbon Nanotube Complex for Biosensing Applications

Chiara Baldacchini, Maria Antonia Herrero Chamorro, Maurizio Prato, Salvatore Cannistraro

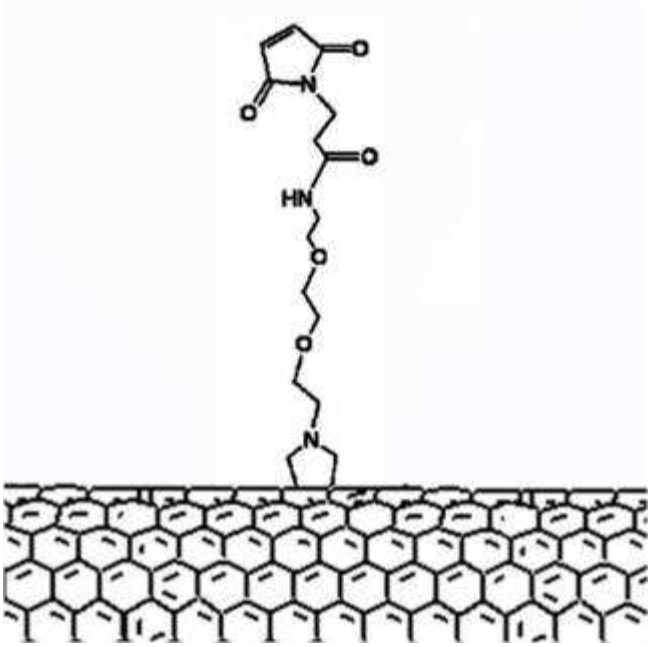

Figure S1: Maleimide-functionalized single-walled carbon nanotubes (Mal-SWNTs). SWNTs (Carbon Nanotechnologies Inc.) have been cut with an acid treatment, and then functionalized *via* cycloaddition to obtain free amino groups uniformly distributed around the sidewalls. The amount of functional groups, as measured with a quantitative Kaiser test, was 260 μmol per gram of material, corresponding to one functional group per 330 C atoms. Considering a C-C distance of 0.11 nm, the Kaiser test indicates a functional group linear density along the SWNTs of about 28 μm^{-1}. The free amino groups have been then derivatized using M-succinimidyl-3-maleimidopropionate (SMP) in dimethyl formamide (DFM), obtaining a uniform distribution of maleimide-terminated chains around the nanotube sidewalls. No amino groups have been revealed by Kaiser test after this procedure, indicating that most of them have reacted.

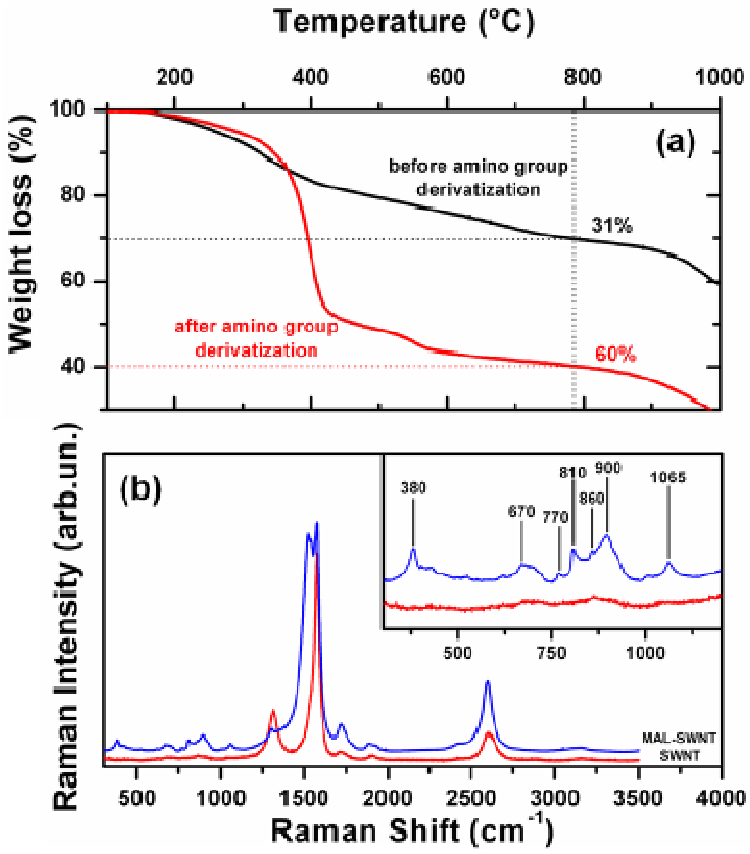

.

Figure S2: Thermo-gravimetric analysis and Raman spectroscopy investigation of Mal-SWNTs. Thermo-Gravimetric Analysis (TGA) has been performed both before and after the amino group derivatization. As shown in panel (a), a higher loss of material has been measured after the SMP linkage, due to the increased molecular weight of the group attached to nanotube sidewalls. The presence of the maleimide-terminated functional chains has been further confirmed by Raman spectroscopy, by comparing the Raman features of Mal-SWNTs with those of pristine SWNTs. Panel (b) shows the Raman spectrum of Mal-SWNTs and that of pristine SWNTs, as obtained by means of a Jobin Yvon LabRAM confocal microspectrometer (spectral resolution < 5 cm^{-1}) equipped with a 1800 grooves/mm grating, a Peltier-cooled CCD detector, and a HeNe 15 mW laser (λ=632.8 nm). The vibrational features of Mal-SWNTs magnified in the inset represent the fingerprints of cycloadded and maleimide rings: the vibrational modes at 670, 770 and 900 cm^{-1} are due to maleimide ring deformation,[S1] and those at 810 and 860 cm^{-1} to the cycloadded pyrrolidine rings (they are absent in the maleimide spectrum[S1] and present in that of SWNTs after cycloaddition, data not shown).

S1 T. Woldbaek, P. Klaboe, C.J. Nielsen, J. Mol. Struct. 1975, 27, 283.

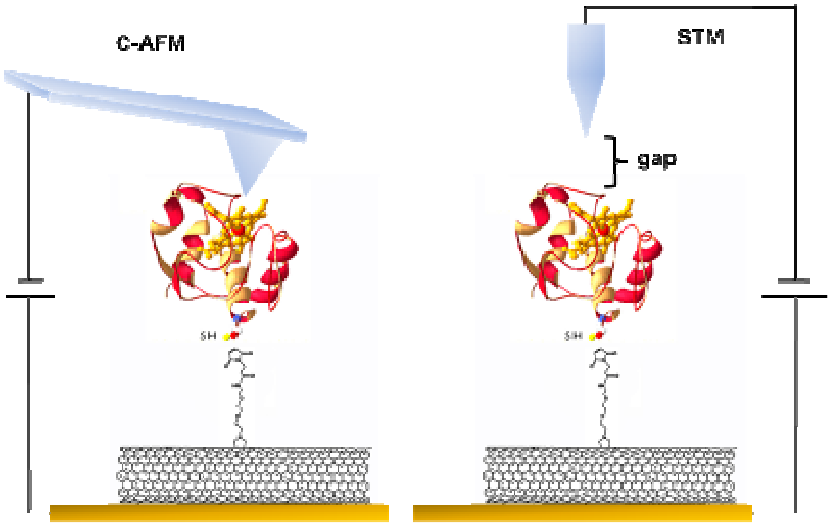

Figure S3: YCC deposition and experimental geometries. To perform single-molecule investigations, Mal-SWNTs have been suspended in DMF (0.2 mg/ml), sonicated for 4 hours, deposited on freshly flame-annealed gold films (Arrandee) by spin-coating (250 µl, 20'' at 2000 rpm), rinsed with ethanol, and dried in pure nitrogen. Then, Yeast Cytochrome c (YCC) molecules have been covalently bound by incubating the samples with a 3µM solution in PBS 40 mM, pH 7.2, for 1 hour at 25°C. YCC has a single exposed cysteine residue, opposite to its haem group, which can be targeted by the maleimide functional termination of the nanotubes, as highlighted in the figure, and this univocally defines the binding geometry. Then, atomic force and scanning tunneling microscopy investigations have been performed on the sample, with the main difference that the AFM tip gets into contact with the surface, while a tunneling gap divides the STM tips from the sample.

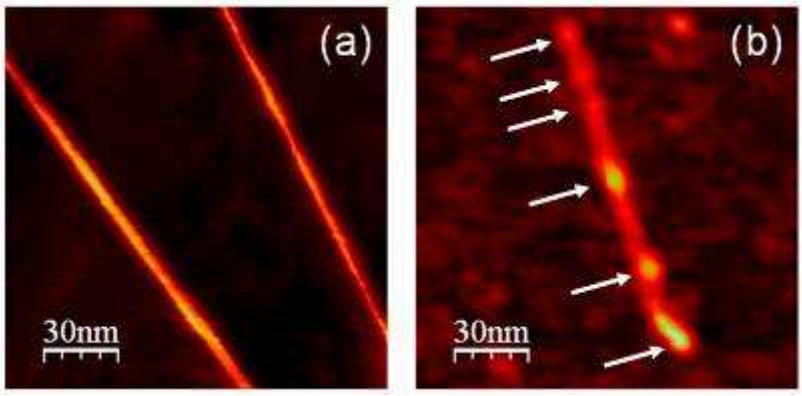

Figure S4. Tapping Mode AFM images (150x150nm^2, color range 3nm) of SWNTs before (a) and after (b) the functionalization with maleimide terminated chains. Pristine nanotube sidewalls are smooth, while Mal-SWNTs present lumps on their sides and ends, indicated by arrows in Figure. These lumps have a mean linear density of 32 ± 11 μm^{-1}, consistent with the functional site density as obtained by Kaiser test (about 28 μm^{-1}). They can be reasonably attributed to single maleimide-terminated chains attached to nanotube sidewalls and these are, to the best of our knowledge, the first high-resolution AFM images of functional sites on SWNT sidewalls obtained without the use of labeling procedures, as instead it is currently done in the literature.[S2-S5]

S2 B.R. Azamian, K.S. Coleman, J.J. Davis, N. Hanson, M.L.H. Green, Chem. Commun. 2002, 366.

S3 K.S. Coleman, S.R. Bailey, S. Fogden, M.L.H. Green, J. Am. Chem.. Soc. 2003, 125, 8722.

S4 L. Zhang, J. Zhang, N. Schmandt, J. Cratty, V.N. Khabashesku, K.F. Kelly, A.R. Barron, Chem. Commun. 2005, 5429.

S5 J. Zhang, L. Zhang, V.N. Khabashesku, A.R. Barron, K.F. Kelly, J. Phys. Chem. C 2008, 112, 12321.